surface, and is electrolyzed. The concentration of free surfactant in the vicinity of the film is kept at less than the cmc so that the film continues to grow for a long period to respectable thicknesses.

Present experiments show that such an electrochemical method serves as a technique for preparing thin films of a wide variety of organic compounds. This technique may enable thin films of organic compounds to be prepared that satisfy the following conditions: (i) the organic compounds are soluble in a micellar solution or dispersible in a surfactant solution and (ii) they are not electrolyzed at the potential for oxidation of the surfactant with a ferrocenyl moiety (+0.3 V vs SCE for FTMA and +0.5 V for FPEG). Another important advantage of this technique is the fact that the starting organic compounds do not undergo electrochemical reactions when their films are formed; hence, film-forming compounds are the same as the starting compounds. Generally, electrochemical film formation proceeds via electrochemical reactions of the starting compounds, and the components of the film-forming compounds are different from those of the starting compounds.

Acknowledgment. We thank R. Ohki for the electron micrograph data. This work was partially supported by a Grant-in-Aid for Scientific Research from the Ministry of Education, Science and Culture (Nos. 62790219, 01604540, and 02205046).

Cysteine Conformation and Sulfhydryl Interactions in Proteins and Viruses. 1. Correlation of the Raman S–H Band with Hydrogen Bonding and Intramolecular Geometry in Model Compounds†

Huimin Li and George J. Thomas, Jr.*

Contribution from the Division of Cell Biology and Biophysics, School of Basic Life Sciences, University of Missouri—Kansas City, Kansas City, Missouri 64110. *Received April 19, 1990*

Abstract: The cysteine sulfhydryl group plays an important role in structural biochemistry. Cysteine thiols of proteins are capable of donating and accepting hydrogen bonds with solvent molecules as well as with other protein groups, and cysteine ligand coordination is fundamental to enzyme activity and nucleic acid recognition. We have undertaken a systematic Raman study of model mercaptans and cysteine thiols to provide an effective spectroscopic probe of the S–H group and its biologically relevant configurations and interactions in aqueous and crystalline proteins. The present study of aliphatic and aromatic mercaptans in both polar and apolar solvents, and of L-cysteine and glutathione in the crystal, provides a basis for interpreting the S–H stretching region of the Raman spectrum in terms of hydrogen bond donation by S–H, hydrogen bond acceptance by S, and rotamer populations of the cysteinyl side chain. The most definitive change observed in the Raman S–H stretching band is its shift to lower frequency when S–H acts as a hydrogen bond donor. We find further that the frequency interval in which the Raman S–H stretching vibration (σ_{SH}) occurs is diagnostic of S–H donors which are strongly hydrogen bonded (2525–2560 cm^{-1}), moderately hydrogen bonded (2560–2575 cm^{-1}), or weakly hydrogen bonded (2575–2580 cm^{-1}). When the S–H group is essentially non-hydrogen-bonded, e.g., at high dilution in CCl_4, we find $\sigma_{SH} \approx 2585 \pm 5$ cm^{-1}. On the other hand, hydrogen bond acceptance by S in the absence of S–H donation elevates σ_{SH} slightly (<4 cm^{-1}). In model mercaptans, P_C and P_H rotamers with respect to the C–C–S–H torsion (χ^2) yield σ_{SH} values that are separated by approximately 10 cm^{-1}, with the P_H rotamer generally exhibiting the higher frequency of the two. Since the S–H region of the Raman spectrum contains no interference from other molecular vibrations, the approximate 10-cm^{-1} shift should be measurable in proteins and thus should provide a means of resolving different cysteine side-chain orientations.

Introduction

Cysteine residues in proteins are capable of a variety of enthalpically favorable polar interactions which presumably contribute to the stabilization of the native structures. Hydrogen bonds involving the sulfhydryl group as donor (S–H···O) or the sulfur atom as acceptor (S···H–N) have been identified from both neutron and X-ray diffraction studies of model compounds (reviewed in ref 1–3). Similar donor-to-acceptor distances determined in protein crystallographic analyses are consistent with sulfhydryl hydrogen bonding in proteins.[4,5] Polar interactions of cysteinyl S and S–H groups with protein aromatic side chains have also been proposed.[6] A common feature of such interactions is the requirement of a shift of electron density from the donor hydrogen toward its covalently bonded sulfur, yielding $^{\delta-}S-H^{\delta+}$ partial charge separation, thereby facilitating favorable interaction at either end of the dipole with an appropriate, oppositely charged group. Thus, a sulfhydryl group that participates in hydrogen bonding or aromatic interaction is expected to exhibit S–H covalency somewhat altered from that of an isolated or noninteracting S–H group. At present, little is known about the energetics of such bonding in proteins and the possible contributing effects of solvent and neighboring protein groups.

The sulfhydryl group of cysteine is also one of the most chemically reactive functional groups in a protein,[7] confirming its nucleophilic nature and the polarity of the sulfhydryl bond. The wide use of sulfhydryl reagents as probes of protein structure and cysteine accessibility underscores the need for additional structural information about interacting S–H groups in proteins, particularly those of aqueous proteins and their assemblies.

† This is paper 32 in the series, Studies of Virus Structure by Raman Spectroscopy. Supported by NIH Grant AI11855.

* To whom correspondence should be addressed.

(1) Taylor, R.; Kennard, O. *J. Am. Chem. Soc.* **1982**, *104*, 5063–5070.
(2) Taylor, R.; Kennard, O. *Acc. Chem. Res.* **1984**, *17*, 320–326.
(3) Burley, S. K.; Petsko, G. A. *Adv. Protein Chem.* **1988**, *39*, 125–189.
(4) Birktoft, J. J.; Blow, D. M. *J. Mol. Biol.* **1972**, *68*, 187–240.
(5) Wilkinson, A. J.; Fersht, A. R.; Blow, D. M.; Winter, G. *Biochemistry* **1983**, *22*, 3581–3586.
(6) Reid, K. S. C.; Lindley, P. F.; Thornton, J. M. *FEBS Lett.* **1985**, *190*, 209–213.
(7) Lundblad, R. L.; Noyes, C. M. *Chemical Reagents for Protein Modification*; CRC Press: Boca Raton, FL, 1984; Vol. I, pp 55–93.

0002-7863/91/1513-456$02.50/0

Table I. Raman Sulfhydryl Group Stretching Frequencies and Bandwidths for Selected Model Mercaptans[a]

	pure liq		CCl_4 soln		acetone[c] soln		water soln	
mercaptan[b]	σ	FWHM	σ	FWHM	σ	FWHM	σ	FWHM
1PT	2570	25.0	2582	17.9	2577	24.2	2578	35.0
2M1PT	2580	26.3	2589	17.1	2586	26.3	2584	28.3
2PT	2570	25.6	2581	16.3	2577	24.4	2572	29.1
2M2PT	2572	22.1	2578	13.3	2576	20.4	2573	27.5
TP	2566	26.0	2584	20.0	2574	35.6	2569	23.3

[a] Raman frequencies (σ) and band full widths at half-maximum (FWHM) are given in cm^{-1} units. [b] Abbreviations: 1PT, 1-propanethiol; 2M1PT, 2-methyl-1-propanethiol; 2PT, 2-propanethiol; 2M2PT, 2-methyl-2-propanethiol; TP, thiophenol. In each of the indicated solvents, the solute concentration is 1% mol/mol. [c] Similar results were obtained for dioxane solutions of 1PT.

Vibrational spectroscopy (Raman or infrared) is often the method of choice for investigating the hydrogen-bonding properties of donor and acceptor groups.[8] Polarization of the donor covalent bond ($^{\delta-}S-H^{\delta+}$) in the presence of an acceptor group, with attendant reduction in the bond force constant, is directly observable in the vibrational spectrum as a shift to lower frequency of the spectral band associated with the S–H bond stretching vibration. In the case of an aliphatic sulfhydryl group, such as that of the cysteine side chain, strong hydrogen bonding is expected to shift the Raman S–H stretching band from the position characteristic of an isolated mercaptan, ca. 2580–2590 cm^{-1}, to values ca. 2530–2540 cm^{-1}, representing a 2% reduction in the vibrational energy of the S–H linkage.[9] Lesser perturbations to the vibration frequency may result from weaker hydrogen bonding or from putative interactions of protein sulfhydryl groups with aromatic rings. The strength of the polar $^{\delta-}S-H^{\delta+}\cdots{}^{\delta-}X$ interaction, by analogy with other types of hydrogen bonding, may be related directly to the magnitude of the S–H vibrational band shift.[8,10,11] Two important advantages have been cited for the use of Raman over infrared spectroscopy in the study of such S–H interactions: (i) the high intrinsic intensity of the Raman S–H stretching band and (ii) the virtual absence of spectral interference from other functional group vibrations in the Raman 2400–2700-cm^{-1} interval.[9]

Previous authors have noted the sensitivity of aliphatic and cysteinyl S–H bonding to different solvent and crystal lattice environments.[12-22] In our structural studies of viruses (reviewed in ref 23), we have shown that the Raman S–H stretching bands of viral coat proteins may vary significantly from one virus to another, thus constituting a potential viral fingerprint, and we have shown that this sulfhydryl signature can also be highly sensitive to deuterium exchange and to changes in pH, ionic strength, or other factors which control virus assembly.[24-27] Up to the present, however, no systematic study has been made of sulfhydryl compounds to correlate the observed Raman S–H band profile with specific cysteine hydrogen-bonding interactions or side-chain conformations in the proteins. Here, we report the results of a systematic model compound study that allows us to propose such a correlation. In this work we have determined the effects of alkyl group branching, chain conformation, and electronegativity of the hydrogen bond acceptor group upon the Raman S–H stretching frequency and band shape.

The present empirical study provides information that is a first step toward understanding S–H interactions in proteins. Elucidation of S–H interactions from protein Raman spectra would complement existing spectra–structure correlations developed for other side chains.[28-33] Future papers in this series will investigate the force field of the cysteine side chain and the hydrogen exchange dynamics of the sulfhydryl group in both model systems and protein crystals of known molecular structure. The availability of reliable spectra–structure correlations is essential to the successful application of Raman spectroscopy in studies of protein structure, folding, and assembly.

Experimental Procedures

1. Materials. The mercaptans ethanethiol (abbreviated ET), 1-propanethiol (1PT), 2-methyl-1-propanethiol (2M1PT), 2-propanethiol (2PT), 2-methyl-2-propanethiol (2M2PT), and thiophenol (TP) were purchased from Aldrich Chemical Co. and were of the highest grades commercially available (1PT, 2M2PT, and TP >99% purity; 2PT >98% purity; 2M1PT >92% purity).

Spectral grade *N,N*-dimethylacetamide (DMA, >99%), diethyl sulfide (DES, >98%), benzene (99%), dioxane (>99%), and *n*-butylamine (>99%) were purchased from Aldrich. Spectral grade (>99%) *n*-heptane, *N,N*-dimethylformamide (DMF), and trifluoroacetic acid were obtained from Sigma Chemical Co. Chemically pure and reagent grade solvents (≥99.5%) were obtained from Fisher Scientific (acetone and CCl_4) and J. T. Baker Chemical ($CHCl_3$).

All mercaptans and solvents were freshly distilled or chromatographed on a 15-cm column of baked alumina gel before use to remove traces of moisture or polar contaminants. The absence of impurities containing hydroxyl, amino, or sulfhydryl groups was verified by Raman or infrared spectroscopy as described.[34] For Raman spectroscopy of mercaptan solutions, the solute was generally dissolved in solvent at nominal concentrations of either 1% or 2% (mol/mol), unless indicated otherwise.

2. Raman Spectroscopy. Raman spectra were excited in the 90° scattering geometry with the 514.5-nm line of a Coherent Innova-70 argon ion laser, using approximately 100 mW of radiant power at the sample. The spectra were recorded on a Spex Ramalog 1401 spectrometer under the control of an IBM microcomputer. Data were collected at intervals of 1.0 cm^{-1}, with an integration time of 1.5 s and spectral slit

(8) Pimentel, G. C.; McClellan, A. L. *The Hydrogen Bond*; Freeman: San Francisco, 1960.
(9) Bellamy, L. J. *The Infrared Spectra of Complex Molecules*, 3rd ed.; Chapman and Hall: London, 1975; Vol. I.
(10) Gordy, W.; Stanford, S. C. *J. Am. Chem. Soc.* **1940**, *62*, 497–505.
(11) Joesten, M. D.; Schaad, L. J. *Hydrogen Bonding*; Dekker: New York, 1974.
(12) Wright, W. B. *Acta Crystallogr.* **1958**, *11*, 632–642.
(13) Hu, S. J.; Goldberg, E.; Miller, S. I. *Org. Magn. Reson.* **1972**, *4*, 683–693.
(14) Kerr, K. A.; Ashmore, J. P. *Acta Crystallogr.* **1973**, *B29*, 2124–2127.
(15) Kerr, K. A.; Ashmore, J. P.; Koetzle, T. F. *Acta Crystallogr.* **1975**, *B31*, 2022–2026.
(16) Bare, G. H.; Alben, J. O.; Bromberg, P. A. *Biochemistry* **1975**, *14*, 1578–1583.
(17) Thomas, G. J., Jr.; Prescott, B.; McDonald-Ordzie, P. E.; Hartman, K. A. *J. Mol. Biol.* **1976**, *102*, 103–124.
(18) Madec, C.; Lauransan, J.; Garrigou-Lagrange, C. *Can. J. Spectrosc.* **1980**, *25*, 47–55.
(19) Byler, D. M.; Susi, H.; Farrell, H. M., Jr. *Biopolymers* **1983**, *22*, 2507–2511.
(20) Itoh, K.; Ozaki, Y.; Mizuno, A.; Iriyama, K. *Biochemistry* **1983**, *22*, 1773–1778.
(21) Rosei, M. A. *Physiol. Chem. Phys. Med. NMR* **1988**, *20*, 189–191.
(22) Pande, J.; McDermott, M. J.; Callender, R.; Spector, A. *Arch. Biochem. Biophys.* **1989**, *269*, 250–255.
(23) Thomas, G. J., Jr. *Biological Applications of Raman Spectroscopy*; Spiro, T. G., Ed.; Wiley-Interscience: New York, 1987; Vol. 1, pp 135–201.
(24) Thomas, G. J., Jr.; Li, Y.; Fuller, M. T.; King, J. *Biochemistry* **1982**, *21*, 3866–3878.
(25) Verduin, B. J. M.; Prescott, B.; Thomas, G. J., Jr. *Biochemistry* **1984**, *23*, 4301–4308.
(26) Prescott, B.; Sitaraman, K.; Argos, P.; Thomas, G. J., Jr. *Biochemistry* **1985**, *24*, 1226–1231.
(27) Li, T.; Chen, Z.; Johnson, J. E.; Thomas, G. J., Jr. *Biochemistry* **1990**, *29*, 5018–5026.
(28) Sugeta, H.; Go, A.; Miyazawa, T. *Bull. Chem. Soc. Jpn.* **1973**, *46*, 3407–3411.
(29) Nogami, N.; Sugeta, H.; Miyazawa, T. *Chem. Lett.* **1975**, 147–150.
(30) Nogami, N.; Sugeta, H.; Miyazawa, T. *Bull. Chem. Soc. Jpn.* **1975**, *48*, 2417–2420.
(31) Ozaki, Y.; Sugeta, H.; Miyazawa, T. *Chem. Lett.* **1975**, 713–716.
(32) Siamwiza, M. N.; Lord, R. C.; Chen, M. C.; Takamatsu, T.; Harada, I.; Matsuura, H.; Shimanouchi, T. *Biochemistry* **1975**, *14*, 4870–4876.
(33) Miura, T.; Takeuchi, H.; Harada, I. *Biochemistry* **1988**, *27*, 88–94.
(34) Thomas, G. J., Jr. *Physical Techniques in Biological Research*, 2nd ed.; Oster, G. F., Ed.; Academic Press: New York, 1971; Vol. 1A, pp 277–346.

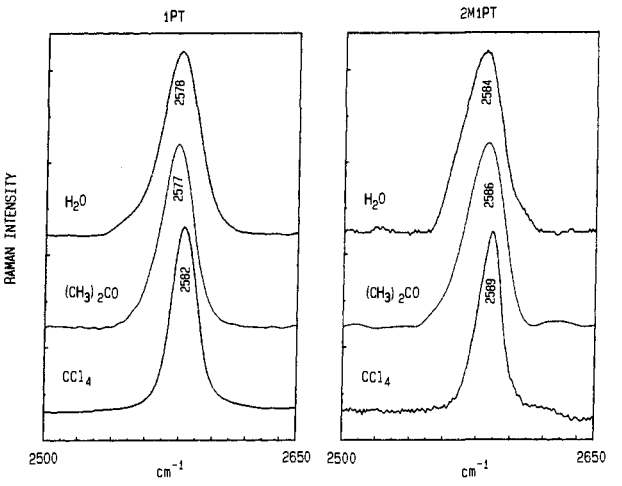

Figure 1. Raman S–H bands of 1% mol/mol solutions of 1-propanethiol (1PT, left panel) and 2-methyl-1-propanethiol (2M1PT, right panel) in CCl_4 (bottom), acetone (middle), and H_2O (top).

width of 8 cm^{-1}. Frequency calibration was performed by measuring the Raman spectrum of indene. The reported Raman S–H and C–S group frequencies are accurate to within ±1 cm^{-1}.

All Raman spectra were recorded at ambient temperature, 25 °C, from samples sealed in glass capillary tubes (KIMAX 34502). Fourier deconvolution of complex band shapes and curve fitting of Raman profiles were carried out by using software developed in our laboratory and previously described.[35,36]

3. Infrared Spectroscopy. FTIR spectra were recorded on a Mattson Instruments Sirius 100 spectrometer. Usually 800 scans each of sample and background were collected at a spectrometer resolution of 8 cm^{-1} and with a triangular apodization function. Samples were contained in a variable-thickness cell with CaF_2 windows.

Results and Discussion

We chose 1-propanethiol (1PT) and 2-methyl-1-propanethiol (2M1PT) as representative of unbranched and branched primary aliphatic thiols. The secondary and tertiary thiols 2-propanethiol (2PT) and 2-methyl-2-propanethiol (2M2PT), respectively, were selected as likely to exhibit steric hindrance to intermolecular association by virtue of their branched carbon chains. The effects of aliphatic chain branching upon vibrational group frequencies are well documented.[9] Thiophenol (TP) was selected as a representative aromatic thiol.

Frequencies and bandwidths of the Raman S–H bands of each of the pure liquid mercaptans are listed in Table I. The S–H stretching frequency is seen to differ considerably among the mercaptans in the neat liquid state. This represents the net effect of a variety of contributing factors, including hydrogen bonding of S–H as donor, hydrogen bonding of S as acceptor, carbon chain branching, gauche/trans configurations with respect to C–C or C–S bonds, and, in the case of TP, interactions of aromatic rings with S and S–H. The separate contributions of these different types of interactions to the observed Raman S–H band frequency and band shape cannot be fully determined in the present empirical approach. However, several factors affecting the Raman S–H band can be delineated by examining selected mercaptans in dilute solutions of appropriate solvents. The results of these investigations are next discussed.

1. Relatively Weak Hydrogen Bonding. Raman spectra of dilute solutions (1% mol/mol) of the representative mercaptans, 1PT and 2M1PT, in CCl_4, acetone, and water are shown in Figure 1. Similar data were collected for all of the model mercaptans, and the complete results are listed in Tables I and II. Although slight differences exist among the mercaptans, all yield the sulfhydryl stretching vibration at or above 2578 cm^{-1} in CCl_4 solution, indicating the virtual absence of intermolecular hydrogen bonding at these experimental conditions.[37]

Table II. Solvent-Induced Shifts of the Raman Sulfhydryl Group Stretching Frequency and Bandwidth[a]

	acetone–CCl_4		water–CCl_4		water–acetone	
mercaptan	δσ	δFWHM	δσ	δFWHM	δσ	δFWHM
1PT	−5	6.3	−4	17.1	+1	10.8
2M1PT	−3	9.2	−5	11.2	−2	2.0
2PT	−4	8.1	−9	12.8	−5	4.7
2M2PT	−2	7.1	−5	14.2	−3	7.1
TP	−10	15.6	−15	3.3	−5	−12.3

[a] Differences of the band peaks (δσ) and bandwidths (δFWHM) for each solvent pair are given in cm^{-1} units. For each solvent pair, the more polar solvent is the minuend. Abbreviations are given in Table I.

Table III. Concentration Dependence of the Raman S–H Stretching Frequency and Bandwidth in Model Compounds[a]

mercaptan	1PT		2M1PT		2M2PT	
concn[b]	σ	FWHM	σ	FWHM	σ	FWHM
0.01	2582	17.9	2589	17.1	2578	13.3
0.10	2581	18.4	2588	18.5	2577	13.7
0.50	2576	20.4	2586	22.9	2575	17.6
0.95	2572	23.8	2581	26.9	2573	21.2
1.00	2570	24.2	2580	27.5	2572	21.8

[a] The center of the Raman S–H stretching band frequency (σ) and the band full width at half-maximum (FWHM) are given in cm^{-1} units for each compound. [b] Mole fraction mercaptan in CCl_4 solution.

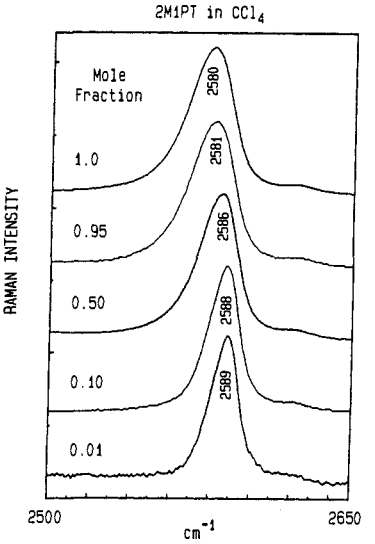

Figure 2. Raman S–H bands of 2M1PT in CCl_4 solutions of solute mole fractions 1.00, 0.95, 0.50, 0.10, and 0.01.

a. Thiol as Hydrogen Bond Donor/Acceptor: Self-Association. Mercaptan sulfhydryl groups are considered incapable of hydrogen bonding at low concentration in nonpolar solvents, such as CCl_4, but do self-associate to form S–H···S bonds as the solute concentration is increased. Similar S–H···S bonds, in which thiols act as both donor and acceptor, occur in the pure liquid.[37] We have examined the Raman spectra of 2M1PT, 1PT, and 2M2PT as a function of thiol concentration in CCl_4 solution. Figure 2 shows the spectra of 2M1PT in CCl_4 for solute mole fractions of 0.01, 0.10, 0.50, 0.95, and 1.00 (neat liquid). Similar data are listed in Table III for 2M2PT and 1PT in CCl_4. We find that both the Raman S–H peak position and the bandwidth [full width at half-maximum (FWHM)] are dependent upon thiol concentration. These results show that S–H···S interactions increase throughout the solute concentration range examined for each thiol in CCl_4 and that S–H···S hydrogen bonding is the dominant factor affecting the peak position and bandwidth. The definitive effect of S–H···S hydrogen bonding is a shift to lower frequency of the Raman S–H band center, which represents the net effect of S–H

(35) Thomas, G. J., Jr.; Agard, D. A. *Biophys. J.* **1984**, *46*, 763–768.
(36) Thomas, G. J., Jr.; Wang, A. H.-J. *Nucleic Acids Mol. Biol.* **1988**, *2*, 1–30.
(37) Bulanin, M. O.; Denisov, G. S.; Pushkina, R. A. *Opt. Spectrosc.* **1959**, *6*, 491–494.

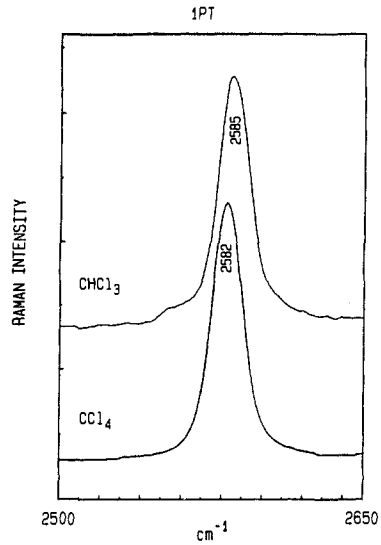

Figure 3. Raman S-H bands of 1% mol/mol solutions of 2M1PT in $CHCl_3$ (top) and CCl_4 (bottom).

donation and S acceptance. [In a later section (5) we show that the population of different rotational conformers does not vary significantly for the mercaptans as a function of concentration in CCl_4.]

Figure 2 also shows evidence of a weak and unresolved low-frequency shoulder to the S-H Raman band of 2M1PT, which gains prominence with increasing X_{SH}. By use of a least-squares algorithm for decomposition of the complex band shape,[38] the data for the neat liquid may be well represented as the composite of a minor Gauss-Lorentz component at 2552 cm^{-1} (14% of total band area, FWHM $\approx$ 26 cm^{-1}) and a major component at 2579 cm^{-1} (86%, FWHM $\approx$ 25 cm^{-1}). The minor component is attributed to higher order multimers of 2M1PT, i.e., association beyond the dimer state. Multimers of hydroxyl compounds, of the type -O-H···O-H···O, are known to contain stronger hydrogen bonding than dimers,[2] and the same is presumed for sulfhydryl associations.

b. Sulfur as Hydrogen Bond Acceptor. To investigate the effect on the Raman S-H band of the S atom acting as an acceptor, we compared Raman spectra of dilute (1%) solutions of 1PT in CCl_4 and $CHCl_3$ solutions. In CCl_4, we expect no hydrogen bonding to the S acceptor; in $CHCl_3$, we expect the C-H donor to form a hydrogen bond to the S acceptor.[37] Figure 3 shows that the Raman S-H band is shifted to *higher frequency* when S accepts the C-H hydrogen; i.e., the peak is shifted from 2582 cm^{-1} in CCl_4 to 2585 cm^{-1} in $CHCl_3$. We also investigated the effect of the much stronger hydrogen bonding donor CF_3COOH on the infrared S-H band of 1PT. We observed again an elevated S-H frequency (2594 cm^{-1}) for the S acceptor and a lowered frequency for the S-H donor (2545 cm^{-1}, data not shown).

2. Moderate Hydrogen Bonding of Thiol as Donor. The investigation of mercaptans in acetone, dioxane, and water solutions permits the determination of spectral characteristics associated with moderate to strong hydrogen bonding of the S-H group. The effects of the aqueous solvent (donor and acceptor) and the acetone or dioxane solvent (acceptor only) are similar but not identical, as seen in Figure 1 and Table I. Although both water and acetone cause a lowering of about 2-9 cm^{-1} in the frequency of the S-H band maximum, as well as substantial band broadening, particularly on the high-frequency side of the band maximum, the effects are somewhat larger in the presence of water than in the presence of acetone. The greater breadth of the S-H band of each aliphatic mercaptan in H_2O presumably reflects the mixed population of both S-H···O and S···H-O hydrogen-bonded species, whereas only S-H···O species are prevalent in the presence of $(CH_3)_2C{=}O$. The exceptional behavior of thiophenol (Table I) probably reflects

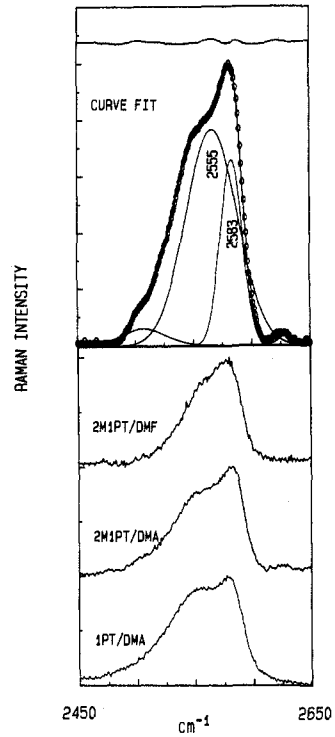

Figure 4. (Bottom) Raman S-H bands of 2% mol/mol solutions of 1-propanethiol (1PT) and 2-methyl-1-propanethiol (2M1PT) in *N,N*-dimethylacetamide (DMA) and for 2M1PT in *N,N*-dimethylformamide (DMF). (Top) Comparison of the observed Raman S-H band (O) of 2M1PT in DMA with its curve-fitted components (—). The fitted profile represents the optimum least-squares fit of the data to four Gauss-Lorentz curves, including two S-H stretching bands (labeled) and two very weak satellites considered to be overtones (unlabeled). The bandwidths and intensities are treated as adjustable parameters in the least-squares convergence.[38] The uppermost trace shows residuals between the observed data and the fitted envelope. Original spectra are corrected for the solvent background.

complex intermolecular interactions between S-H and the phenyl ring.

When the hydrocarbon chain is unbranched, the broadening effect caused by H_2O on the Raman S-H band is substantially greater than that caused by acetone, as illustrated by a comparison of the data for solutions of 1PT and 2M1PT shown in Figure 1. The greater broadening effect of H_2O for the unbranched thiol (1PT) is consistent with the expectation that O-H donor groups of H_2O form more extensive hydrogen bonds to thiol S acceptors in the absence of chain branching.

The trends noted above are preserved throughout the series of compounds studied (Table II). Thus, the extent of S-H hydrogen bonding is sensitive to the steric effects imposed by the hydrocarbon chain, and this is reflected in the shape of the Raman S-H band.

3. Relatively Strong Hydrogen Bonding of Thiol as Donor. Thermodynamic data for hydrogen bonding of thiols with *N,N*-dimethylacetamide (DMA) and *N,N*-dimethylformamide (DMF) have been reported.[13,39] The results confirm that thiols form much stronger hydrogen bonds with carbonyl acceptors of DMA and DMF than with acetone. To observe effects of relatively strong S-H···O hydrogen bonding upon the Raman S-H band, we have investigated the spectra of 1PT and 2M1PT in DMA and DMF solutions (2% mol/mol). Representative data are shown in Figure 4, indicating a complex band shape comprising a main peak centered near 2580 cm^{-1} and partially resolved broad shoulder near 2555 cm^{-1}. The complex band may be well represented as the composite of a broad Gauss-Lorentz component at 2555 cm^{-1} (FWHM $\approx$ 60 cm^{-1}) and narrower component at 2583 cm^{-1}

(38) Sugeta, H. *Bull. Chem. Soc. Jpn.* **1981**, *54*, 3706-3710.

(39) Copley, M. J.; Marvel, C. S.; Ginsberg, E. *J. Am. Chem. Soc.* **1939**, *61* (2), 3161-3162.

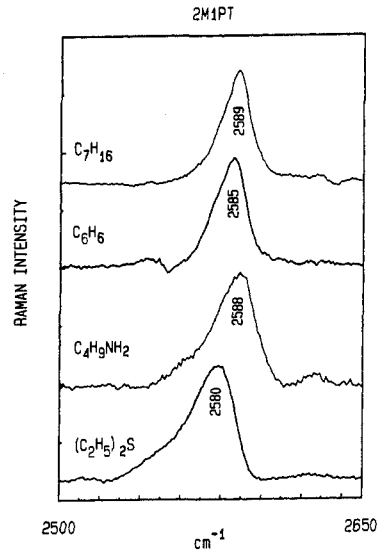

Figure 5. (From top to bottom) Raman S–H bands of 2% mol/mol solutions of 2M1PT in heptane, benzene, *n*-butylamine, and diethyl sulfide.

(FWHM ≈ 25 cm^{-1}), as illustrated for the DMA solution of 2M1PT in the upper panel of Figure 4. Identical results were obtained for DMF. A similar low-frequency component was observed for CF_3COOH solutions (data not shown).

We assign the broad major band of lower frequency to the strongly hydrogen bonded S–H groups and the narrow minor band of higher frequency to S–H groups not forming strong hydrogen bonds. Sulfhydryls of the former type are expected to yield S—H···O=C bonds, while the latter may include S—H···$N(CH_3)_2$ bonds as well as non-hydrogen-bonded sulfhydryls. If this interpretation is correct, we expect a sulfhydryl band to occur also near 2585 cm^{-1} in amine solutions of thiols. We have confirmed that 2M1PT and other thiols exhibit a band centered near 2580–2588 cm^{-1} in *n*-butylamine solutions (see section 4). Also, we expect that in DMA solutions of thiols the Raman intensity of the shoulder ca. 2545–2555 cm^{-1} should decrease at the expense of the peak ca. 2580 cm^{-1} as the strong S—H···O=C hydrogen bonding is disrupted with increasing temperature. Evidence of such an intensity shift with temperature is observed for both 1PT and 2M1PT (data not shown), in accordance with the proposed interpretation. The relevance of this result to strong S—H···O=C hydrogen bonding in peptide analogues will be discussed below.

4. Other Solvents. To mimic the molecular environments of cysteine sulfhydryl groups in proteins, we have collected the Raman spectra of mercaptans in additional solvents. Diethyl sulfide (DES) was chosen to represent the environment of the methionine (Met) side chain, *n*-butylamine (NBA) for side-chain NH_2 groups (Lys, Arg, Gln, Asn), benzene for aromatic side chains, and *n*-heptane for aliphatic side chains. The results are shown in Figure 5.

For 2M1PT in NBA (2% mol/mol), the half-width of the Raman S–H band is increased by 7 cm^{-1} compared to the CCl_4 solution (cf. Figure 1), with little change in peak position (2588 cm^{-1}). The increase of bandwidth clearly indicates solute–solvent interaction, i.e., hydrogen bond formation. Since the acceptor role of the sulfhydryl S atom would tend to elevate the S–H frequency (section 1.b.) and the donor role would tend to lower frequency (section 1.a.), the observed invariance of the Raman peak position in NBA vis-à-vis CCl_4 may reflect the compensating effects of S–H hydrogen bonding as both donor (to amino N) and acceptor (from amino NH). Figure 5 also shows that the low-frequency shoulder of the Raman S–H band is centered near 2560 cm^{-1}, not as low as expected for strong S–H hydrogen bonding to C=O (section 3.). We conclude that S–H forms both donor and acceptor interactions with primary amino groups but that these interactions are relatively weak in comparison to S–H interactions with carbonyl acceptors.

For 2M1PT in DES (2% mol/mol), a broader and more asymmetric band shape is observed, with substantial lowering of the major peak position (2579 cm^{-1}) when compared with the CCl_4 solution spectrum (2589 cm^{-1}). This reflects the predominance of S–H donor interactions with solvent S acceptors. The position of the major peak indicates clearly that the S–H···S hydrogen bonding is relatively weak in solution. Surprisingly, a low-frequency shoulder (ca. 2552 cm^{-1}) to the major band is also apparent in the DES solution of 2M1PT. In the absence of strong hydrogen bond acceptors, and by analogy with the neat liquid (section 1.a.), this feature may indicate the 2M1PT sulfhydryl in three-center association with two DES molecules of the type

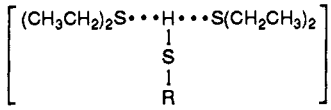

Investigations of aryl and arylalkyl mercaptans have been carried out previously,[3,40,41] although Raman S–H frequencies for cysteine analogues in aromatic solvents have not been studied. To determine the Raman S–H frequency characteristic of S–H···ϕ interaction, we have obtained the spectrum of 2M1PT in benzene (2% mol/mol) shown in Figure 5. The S–H Raman band is relatively symmetric and centered at 2585 cm^{-1}, lowered by 4 cm^{-1} from the value observed in the CCl_4 solution. This frequency shift may be taken as evidence of S–H interaction with the partial negative center axial to the aromatic ring.[3] We note also that the Raman band is sharp (FWHM = 19.5 cm^{-1}) and on this basis may be clearly delineated from the much broader band (FWHM = 28.5 cm^{-1}) of similar frequency for 2M1PT in H_2O solution.

For 2M1PT in heptane (2% mol/mol), the Raman S–H band is sharp (FWHM = 17.5 cm^{-1}) and centered at the identical frequency observed for the CCl_4 solution (2589 cm^{-1}). This indicates no S–H interactions in the alkane environment.

5. Effect of Rotamer Population. To complete our correlation of the Raman S–H stretching frequency (σ_{SH}) with sulfhydryl interaction, it is appropriate to assess possible effects of molecular conformation on the vibrational band frequency. This is particularly important for applications to proteins, since the cysteine side chain is capable of rotations about Cα–Cβ and Cβ–S bonds (torsion angles χ^1 and χ^2, respectively). [Note that we use here the notation appropriate to protein side-chain substituents; i.e., Cα represents the peptide main-chain carbon (α to the peptidyl C=O group), and Cβ represents the cysteinyl side-chain carbon (β to the peptidyl C=O group).] Changes in the torsion angle χ^1 are not expected to affect σ_{SH} to a large extent, since the S–H stretching vibration is highly localized and presumably involves only very minimal mechanical coupling with motions of the Cα substituents including its Cα–Cβ bond. However, changes in the torsion angle χ^2 may affect σ_{SH} significantly, in view of the known barrier to internal rotation about Cβ–S in simple aliphatic mercaptans.[42,43] In addition, configurational changes in the cysteine side chain may alter steric access of other polar or polarizable groups, thus indirectly affecting the frequency of the Raman S–H band. We have investigated these effects in CCl_4 solution spectra of the mercaptans 1PT, 2PT, 2M1PT, and 2M2PT. For 1PT and 2M1PT, the solution conformations about the Cα–Cβ bond are known from correlations established between Raman C–S stretching band frequencies and intensities and rotamer types and populations.[28-31,44,45]

The Raman spectra of CCl_4 solutions of 1PT, 2PT, and 2M1PT show an *unsymmetric* S–H band, whereas 2M2PT shows a *symmetric* S–H band (Figure 6). The former three compounds are

(40) Saunders, R. H.; Murray, M. J.; Cleveland, F. F. *J. Am. Chem. Soc.* **1942**, *64*, 1230–1231.
(41) Alencastro, R. B. D.; Sandorfy, C. *Can. J. Chem.* **1972**, *50*, 3594–3600.
(42) Durig, J. R.; Bucy, W. E.; Wurrey, C. J.; Carreira, L. A. *J. Phys. Chem.* **1975**, *79*, 988–993.
(43) Richter, W.; Schiel, D. *Chem. Phys. Lett.* **1984**, *108*, 480–483.
(44) Hayashi, M.; Shiro, Y.; Murata, H. *Bull. Chem. Soc. Jpn.* **1966**, *39*, 112–117.
(45) Scott, D. W.; El-Sabban, M. Z. *J. Mol. Spectrosc.* **1969**, *30*, 317–337.

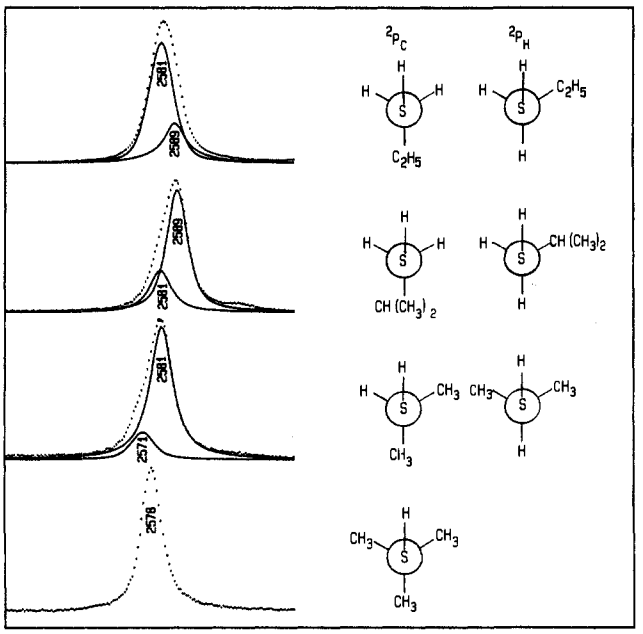

Figure 6. (Left, from top to bottom) Raman S–H bands of 2% mol/mol solutions of 1PT, 2M1PT, 2PT, and 2M2PT in CCl_4. For each mercaptan the observed Raman S–H band (···) is compared with its curve-fitted components (—). (Right) Newman projection formulas for rotamers ^2P_H and ^2P_C, with respect to the torsion angle χ^2 defined in the text. In each case, the more intense Raman S–H band is assigned to the ^2P_H rotamer, in accordance with ethanethiol.[42]

capable of rotational isomerism with respect to the Cα–Cβ–S–H network (torsion angle χ^2); the latter is not. Accordingly, a logical explanation for the difference in Raman S–H band shapes is the difference in rotamer populations about the Cβ–S bond. In the case of each unsymmetric Raman S–H band (1PT, 2PT, 2M1PT), the σ_{SH} envelope can be decomposed into an intense component and a weak component, presumably reflecting the two inequivalent rotamers, ^2P_C (Cα trans to SH; here, the superscript signifies rotation with respect to torsion χ^2) and ^2P_H (CβH trans to SH), as shown in Figure 6. The assignment scheme of Figure 6 is consistent with the data obtained from the gas-phase vibrational spectra of ethanethiol, which also exhibits two rotamers.[42,43] For each resolved band shape in Figure 6, we find the two components (corresponding to rotamers ^2P_C and ^2P_H) separated by 8–10 cm^{-1}, consistent with the 9-cm^{-1} difference reported for ethanethiol.[42]

It is important to note that the vibrational spectrum, though capable of resolving different rotamers, may not provide unambiguous assignments for them. However, we follow here (Figure 6) the assignment scheme of Durig et al.,[42] deduced from the calculated torsional barrier (1.41 kcal/mol), which indicates that the gauche positioning of S and Cα (^2P_H) represents a lower energy configuration than the gauche positioning of S and Hβ (^2P_C). Thus, in Figure 6, the more intense Raman S–H band is assigned in each case to the ^2P_H rotamer and the minor band to the ^2P_C rotamer. We are currently pursuing normal coordinate calculations to further test and refine this model.

Raman spectra of 2M1PT and 1PT (neat liquids) display two bands in the C–S stretching region (600–800 cm^{-1}), indicating an equilibrium of two rotamers for each mercaptan. With regard to the Cα–Cβ torsion (χ^1), the data (not shown) indicate for 2M1PT a prevalence of ^1P_C (712-cm^{-1} marker) over ^1P_H (672-cm^{-1} marker), as reported previously.[31] For 1PT, corresponding assignments indicate that the ^1P_H conformation (650 cm^{-1}) prevails greatly over ^1P_C (704 cm^{-1}). If we assume that the Raman scattering cross sections are roughly the same for each rotamer, the data indicate $^1P_H/^1P_C$ ratios of 1/2 for 2M1PT and 4/1 for 1PT, i.e., an 8:1 difference between the two mercaptans. This large difference in Cα–Cβ rotamer populations may lead to significantly different accessibilities of hydrogen bonding acceptor groups to the respective S–H donors of 1PT and 2M1PT. This may account for the different σ_{SH} values observed for 1PT and

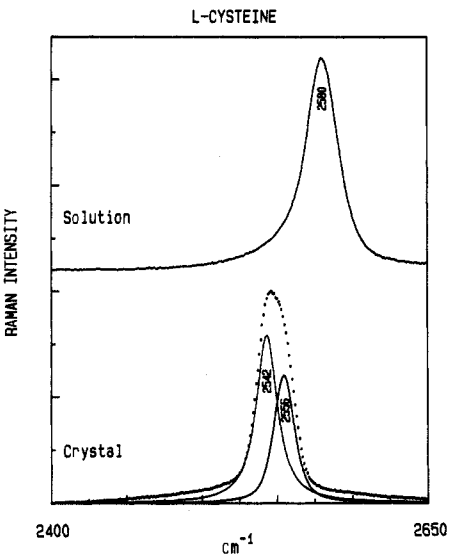

Figure 7. Raman S–H bands of L-cysteine. (Top) Data for 1% mol/mol solution in H_2O at pH 7. (Bottom) Data for the orthorhombic crystal[15] (···) and its curve-fitted components (—).

2M1PT liquids and solutions (Table I). For example, we observe $\delta(\sigma_{SH})$ between 2M1PT and 1PT liquids of approximately 10 cm^{-1}, while $\delta(\sigma_{SH})$ between 2M1PT and 1PT solutions is about 8 cm^{-1}. This value of $\delta(\delta(\sigma_{SH})) = 2$ cm^{-1} suggests that the dominant ^1P_H conformation of 1PT may facilitate S–H···S hydrogen bonding.

In any case, Raman spectroscopy provides an ideal probe of the local molecular conformation in these cysteine model compounds. The C–S stretching region is sensitive to torsion angle χ^1, while the S–H stretching region is informative of χ^2.

6. Effects of Steric Hindrance. Finally, we note that observed shifts of σ_{SH} with solute concentration for different mercaptans in CCl_4 (Table I) are consistent with the anticipated steric effects of carbon chain methylation upon associative interaction. Thus, 1PT with the least steric hindrance, exhibits the largest σ_{SH} hydrogen bonding shift (12 cm^{-1}). For 2M2PT, with the most steric hindrance, the σ_{SH} shift is least (6 cm^{-1}); for 2M1PT, it is intermediate (9 cm^{-1}).

Similar rules apply to access of the hydrogen bonding solvent, acetone, to mercaptan S–H groups. Table II shows that 1PT suffers the largest hydrogen bonding shift (5 cm^{-1}) and 2M2PT the lowest (2 cm^{-1}) in the presence of acetone. On the other hand, the water molecule is exceptional. Due to its smaller molecular size, H_2O is apparently not obstructed by α-methyl substituents from hydrogen bonding with the thiol group (Table II).

7. Comparison of σ_{SH} in Crystal and Solution Structures of Protein Model Compounds: Cysteine and Glutathione. X-ray and neutron diffraction studies of orthorhombic L-cysteine show that the four cysteinyl sulfhydryl groups in the crystallographic unit cell are "disordered" and are involved in short contacts with both sulfur and carbonyl oxygen, implying relatively strong hydrogen bonds of the type S—H···S and S—H···O=C.[14,15] Neutron diffraction results indicate that the S–H covalent bond length is longer in the case of the S–H···S contact (1.45 Å) than in the case of the S–H···O contact (1.36 Å) and also that the H···acceptor contraction is greater for S–H···S, implying that the S–H···S contact is the stronger of the two.[15] Although this is the opposite of what would be expected on the basis of acceptor electronegativities, Kerr et al.[15] point out that the carbonyl group is shared with two other hydrogen bond donors, thus reducing its availability as an S–H acceptor. (The S–S and S–O distances are, respectively, 3.79 and 3.41 Å.) We show the Raman spectrum of the orthorhombic L-cysteine crystal in Figure 7 (bottom). A complex band appears at 2550 cm^{-1}, which can be decomposed into two Gauss–Lorentz components of nearly equal intensities at 2542 and 2556 cm^{-1} (Figure 7, bottom). On the basis of the neutron diffraction results,[15] we propose the assignment of the lower frequency component (2542 cm^{-1}) to the longer S–H bond, i.e.

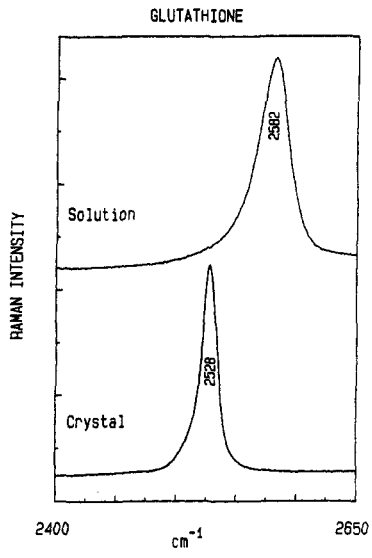

Figure 8. Raman S-H bands of glutathione. (Top) Data for 1% mol/mol solution in H_2O at pH 7. (Bottom) Data for the orthorhombic crystal.[12]

S-H···S. The results in Figure 7 show that both S-H···S and S-H···O interactions in the crystal state may lead to very low S-H stretching frequencies, comparable to the lowest values observed in the solution state (cf. Figure 4). Figure 7 (top) also shows that L-cysteine in aqueous solution (1% mol/mol) exhibits σ_{SH} at 2580 cm^{-1}, typical of an unbranched mercaptan hydrogen bonded to the H_2O acceptor (cf. Figure 1).

Figure 8 shows that σ_{SH} in the crystal state may be lowered well below even the lowest value observed for solutions. In the orthorhombic crystal of the naturally occurring tripeptide glutathione (γ-L-glutamyl-L-cysteinylglycine), σ_{SH} occurs as a relatively sharp band at 2528 cm^{-1}. The low value of σ_{SH} in glutathione may be attributed to the simultaneous formation of four strong S-H···O hydrogen bonds to carboxyl and carbonyl oxygens with S-O distances of 3.53, 3.57, 3.63, and 3.90 Å.[12] In a 1% (mol/mol) aqueous solution of glutathione, σ_{SH} occurs as a broad band at 2582 cm^{-1} (Figure 8).

Conclusions

The present empirical analysis shows that the Raman S-H band in simple mercaptans is typically complex and is influenced significantly both by solvent environment and by intramolecular conformation. Despite these complexities, analysis of the Raman S-H band profile in a variety of solvents and over wide ranges of concentration and temperature permits certain conclusions to be reached regarding factors that elevate or lower the band frequency and alter the spectral band shape. These conclusions appear to be relevant to ascertaining cysteine S-H group environment and interaction in proteins.

The major conclusions of this work are the following:

(1) The Raman S-H stretching band (σ_{SH}) exhibits a significant shift to lower frequency with participation of the S-H donor group in hydrogen bond formation in the solution state. For different propyl mercaptans, which serve as models for the cysteine side chain in proteins, we have measured the shift of σ_{SH} upon transferring the thiol group from the non-hydrogen-bonded state (dilute CCl_4 solution) to various *donor* hydrogen-bonded states (acceptor solvents). In the absence of hydrogen bonding, σ_{SH} occurs for all mercaptans in the interval 2578–2589 cm^{-1}. The average σ_{SH} shift is –4 cm^{-1} with hydrogen bonding to the acetone carbonyl acceptor [S—H···O=C$(CH_3)_2$], –6 cm^{-1} with hydrogen bonding to H_2O (net effect of S—H···OH_2 and H–O–H···S—H interactions), –30 cm^{-1} with hydrogen bonding to substituted amides (S—H···O=CNR_2), and –40 cm^{-1} with hydrogen bonding to trifluoroacetic acid [S—H···O=C(OH)CF_3]. Note that although some hydrogen-bonded S-H groups may also yield σ_{SH} in the interval 2578–2589 cm^{-1}, these are clearly differentiated from the non-hydrogen-bonded states by the much greater width of their Raman S-H bands (Tables I and II).

(2) The σ_{SH} bands of both free and donor thiol groups can also be distinguished in spectra of CCl_4 solutions as a function of mercaptan concentration. For concentrated solutions of the same model mercaptans discussed above, σ_{SH} shifts on average –9 cm^{-1} when the thiol is hydrogen bonded as donor to the S acceptor (S-H···S). The observed sigmoidal shape of the plot of σ_{SH} versus thiol mole fraction in CCl_4 solution indicates higher order associations at high thiol concentrations and compensating effects of decreasing and increasing frequency shifts induced, respectively, by donor and acceptor roles (H. Li and G. J. Thomas, Jr., unpublished work). At conditions favoring higher order multimers, the Raman S-H band exhibits asymmetry on its low-frequency side which can be accounted for by a weak satellite near 2552 cm^{-1}.

(3) The Raman S-H stretching band undergoes a small shift to higher frequency when the S atom acts exclusively as the *acceptor* of a hydrogen bond. In $CHCl_3$ solution, the unbranched propyl mercaptan (1PT) exhibits a 3-cm^{-1} shift of σ_{SH} to higher frequency.

(4) When the conformation of the Cα–Cβ–S–H group is changed from ^2P_C (Cα trans to H) to ^2P_H (Hβ trans to H), the S-H frequency changes by about 8–10 cm^{-1}. In all but one case (1PT), the ^2P_H rotamer exhibits the higher frequency. This may reflect a tendency toward greater electron induction into the sulfhydryl bond when alkyl groups are gauche to S-H. To a lesser extent, mechanical coupling of σ_{SH} with skeletal modes may also influence the rotamer frequencies. We note that gas-phase Raman spectra of rotamers of ethanethiol provide some evidence for mechanical coupling in the case of the two-carbon chain.[43] Further studies are in progress to resolve the mechanical coupling effects in cysteine models more definitively.

(5) The shorter H···acceptor contacts and stronger hydrogen bonding permitted for the solid state can lead to much lower values of σ_{SH} than observed for the solution state. Raman data obtained on orthorhombic L-cysteine and orthorhombic glutathione crystals, for which high-resolution structure information is available, indicate a range of 2525–2560 cm^{-1} for strong S-H hydrogen bonding in the crystal. The data also indicate that comparably strong S-H hydrogen bonding to S and O acceptors leads to comparable lowering of σ_{SH} in the cysteine crystal. Further investigation of S-H hydrogen bonding in the crystal will be carried out to determine whether σ_{SH} can be correlated directly with the length of the H···acceptor contact.

Acknowledgment. Support of the National Institutes of Health (Grant AI11855) is gratefully acknowledged. We also thank Prof. Charles Wurrey, Department of Chemistry, for many helpful suggestions and for his interest and assistance throughout all phases of this project. This work constitutes part of the M.S. thesis research of H. Li.